# Observation of a Highly Excited Long-Lived Valence State in $H_2$

E. Reinhold, W. Hogervorst, and W. Ubachs

*Laser Centre, Department of Physics and Astronomy, Vrije Universiteit, De Boelelaan 1081, 1081HV Amsterdam, The Netherlands*

(Received 30 December 1996)

We present the first observation of a long-lived valence state of $H_2$ close to the ionization threshold, populated in a double resonance laser excitation scheme with extreme ultraviolet radiation in the first step. Level energies of rovibrational states, confined in the outer part of the double-well $H\overline{H}\,^1\Sigma_g^+$ potential at a large internuclear distance of 11 a.u., have been determined with an accuracy of 0.04 $cm^{-1}$. Observed weak autoionization, increasing with vibrational energy, is explained by tunneling through the potential barrier. [S0031-9007(97)02829-9]

PACS numbers: 33.70.Ca, 31.50.+w, 33.80.Eh, 34.30.+h

The binding of atoms in diatomic molecules usually leads to configurations where the internuclear separation nearly equals the sum of the atomic radii. Molecules in excited valence states for which the binding at the outer limb of the potential becomes ionic, such as in the $B^1\Sigma_u^+$ state of the hydrogen molecule, including its isotopomers, and the $B^1\Sigma^+$ state of HF [1], show larger interatomic separations. However, such states are represented by a single-minimum potential energy curve and, consequently, the wave function density is at least partly located at short distance. Avoided crossings between diabatic states with the same reflection and inversion symmetry, multiplicity, and orbital angular momentum can give rise to double-well structures in the corresponding adiabatic representation of potential curves. A well-known example is the $EF^1\Sigma_g^+$ state in the hydrogen molecule [2] with a second minimum at 4.4 atomic units (a.u.). At energies below the potential barrier both wells can be considered in approximation separately with their own sets of energy levels, which may be perturbed by resonant tunneling [3].

In the potential of the fourth $^1\Sigma_g^+$ state in hydrogen, called the $H\overline{H}$ state, a barrier, and a second well are formed in the same way. The outer well of $H\overline{H}$ is created by the crossing of a repulsive H(1$s$) + H(2$p$) Heitler-London configuration with the $H^+ + H^-(1s)^2$ ion-pair configuration. The outer well part and its energy levels are denoted briefly as $\overline{H}$ in the following. Its broad potential minimum is located at an internuclear separation as large as 11 a.u. and at an energy of 15 eV above the ground state of $H_2$, just 0.22 eV below the ionization threshold. In a series of papers Wolniewicz and Dressler [4–6] reported *ab initio* calculations of the potential of the $H\overline{H}\,^1\Sigma_g^+$ state and the energy levels of the various isotopes. In the case of $H_2$ the $\overline{H}$ state must contain 16 vibrational levels below the top of the potential barrier, part of which are located above the ionization threshold ($v \geq 5$). For the latter states the autoionization rate remains low because tunneling through the broad potential barrier is necessary to reach the internuclear distance of the electronic ground state of $H_2{}^+$. In addition the states confined to the outer well are predicted to predissociate with a very small rate, so they are expected to decay predominantly radiatively at an estimated rate of $7 \times 10^6$ $s^{-1}$, corresponding to a lifetime of 140 ns [4].

In this Letter we report the observation of 14 vibrational levels of the $\overline{H}\,^1\Sigma_g^+$ state in $H_2$, in a double resonance study employing a tunable extreme ultraviolet (XUV) laser in combination with a visible laser. The $\overline{H}$ levels were excited by electric dipole transitions from high $v$ levels of the $B^1\Sigma_u^+$ state, having appreciable Franck-Condon overlap at the outer limb of the $B$-state potential. The intermediate $B$ levels were prepared in excitation from the $X^1\Sigma_g^+, v = 0$ ground state with Franck-Condon overlap at short internuclear distances (see Fig. 1 for excitation scheme). The XUV-laser setup as well as its application to high resolution spectroscopy of $H_2$ have been described earlier [7]. The required XUV radiation at 91.5 nm for the $B$-$X$ transition was generated by frequency doubling in a KD*P crystal the output of a pulsed dye laser at 550 nm, pumped by the second harmonic of an injection-seeded Nd:YAG laser, and subsequently generating the third harmonic by focusing the UV into a gas jet. The XUV radiation was separated from the incident UV using noncollinear phasematching, such that no UV fundamental was present in the excitation region. The XUV source was tuned to selected rovibrational $B$ levels and remained fixed. A second dye-laser pulse was counterpropagated through the interaction region, overlapping in time with the XUV pulse. Its wavelength was scanned over the transitions to several $\overline{H}, v$ levels in the range 556–735 nm. To produce ions for signal registration of the $\overline{H}$-$B$ resonances a third laser pulse at 355 nm (third harmonic of the Nd:YAG) was used. This pulse was delayed by 15 ns relative to the first two pulses to avoid ionization of the (short-lived) $B$ state. Ions were extracted using a pulsed electric field and detected with an electron multiplier, monitoring $H_2{}^+$ and $H^+$ ions separately in a time-of-flight setup.

$P(1), R(0), R(1), R(2)$, and $R(3)$ transitions of the $B$-$X$ (18,0) and (19,0) bands were used to prepare $J = 0$ to 4 levels, from which $\overline{H}$ levels ranging from $v = 2$ up to

  

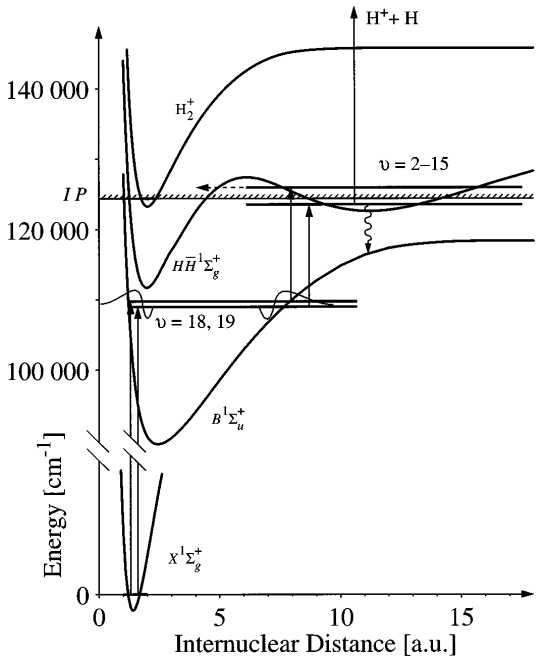


FIG. 1. Potential energy curves of states in $H_2$ relevant for the excitation scheme. The $\overline{H}^1\Sigma_g^+$ (outer well) states are populated in a XUV-visible double-resonance laser process via intermediate $B^1\Sigma_u^+$, $\upsilon = 18$, 19 levels. A delayed laser pulse further excites the $\overline{H}$ states to produce $H^+$ for signal recording. The dashed arrow indicates autoionization via tunneling through the $H\overline{H}$ barrier.

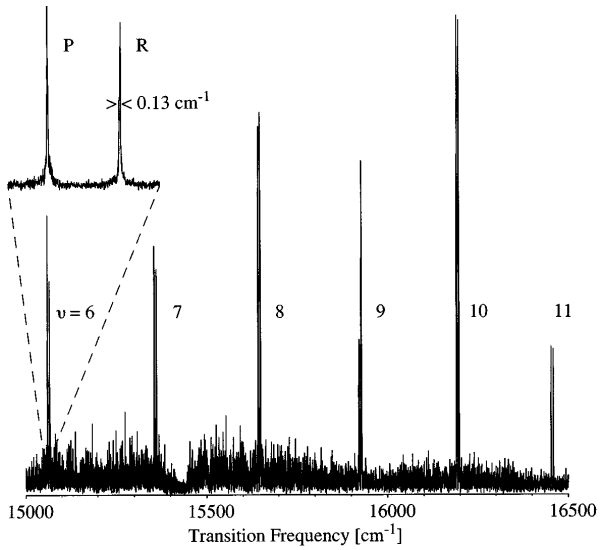


FIG. 2. Spectrum of $\overline{H}^1\Sigma_g^+$-$B^1\Sigma_u^+$ transitions, taken with $B$, $\upsilon = 19$, $J = 1$ as intermediate state and scanning the second laser over the range 600–670 nm while recording the $H^+$ signal. $P$ and $R$ transitions to $J = 0$ and $J = 2$ of a vibrational level are separated by about 6 cm$^{-1}$. The inset displays a shorter, high resolution scan, showing some broadening beyond the laser linewidth of 0.06 cm$^{-1}$ due to saturation.

the maximum of $\upsilon = 15$ with $J = 0$ to 5 were excited. The $\upsilon = 0$ and $\upsilon = 1$ levels were not measured due to technical problems. An overview spectrum is shown in Fig. 2, using the $B^1\Sigma_u^+$ $\upsilon = 19$, $J = 1$ as intermediate state and recording the signal of $H^+$ produced by the delayed UV-pulse. It displays transitions to the $\upsilon = 6$–11 vibrational $\overline{H}$ states with a spacing decreasing from about 300 to 260 cm$^{-1}$ and the characteristic doublet structure of a $^1\Sigma_u^+$-$^1\Sigma_g^+$ transition with the $P$ and $R$ lines separated by 6 cm$^{-1}$. The inset in Fig. 2 shows an example of a detailed high resolution scan. At sufficiently low power in the second step to avoid saturation broadening (between 1 mJ and 7 $\mu$J per pulse depending on the transition strength) a laser bandwidth determined resolution of about 0.06 cm$^{-1}$ was reached. Calibration of $\overline{H}$-$B$ transition frequencies in the 556 to 675 nm range was performed by simultaneously recording an $I_2$-absorption spectrum, leading to an accuracy of 0.01 cm$^{-1}$ [8]. For longer wavelengths optogalvanically detected argon lines were used for reference, resulting in an accuracy of only 0.1 cm$^{-1}$. Energies of the rovibrational $\overline{H}$ levels were determined by adding the energies of the rotational ground state levels [9] and of the $B$-$X$ transitions [7] to the measured $\overline{H}$-$B$ transition energies, leading to uncertainties of 0.04 cm$^{-1}$ on average. Combination differences between $P$ and $R$ transitions as well as via $B$, $\upsilon = 18$ and 19 intermediate states were verified and led to improved accuracy.

A rotational analysis was made to derive band origins $T_\upsilon$ and rotational constants $B_\upsilon$. Experimental energies fit the relation $E = T_\upsilon + B_\upsilon J(J + 1)$ for a rigid rotor within their uncertainties, except for $\upsilon = 14$, $J = 3$ and 4, which will be discussed later. This indicates that the $\overline{H}$ state is unperturbed, in contrast to the large number of other mutually interacting states in this energy region. In Table I band origins $T_\upsilon$ are compared with the values calculated by Wolniewicz and Dressler [5], showing reasonable agreement. Extrapolation of the deviations in $T_\upsilon$ leads to an estimate of the potential minimum that is 12.5 cm$^{-1}$ lower than the calculated value. $T_\upsilon$ values could in principle be used to derive a zero-point vibration frequency $\omega_e$ and an anharmonic constant $\omega_e x_e$ to be used in an anharmonic potential model, but in view of the accurate *ab initio* calculations this would not give more insight. Internuclear separations $R_\upsilon$ corresponding to the $B_\upsilon$ constants (listed in Table I), using the relation $B_\upsilon = h/(8\pi^2 c\mu R_\upsilon^2)$ in the rigid rotor model, are found to decrease with increasing $\upsilon$ as predicted, contrary to the usual behavior in an anharmonic single-well potential (Fig. 3). The equivalent expectation values $\langle R^{-2}\rangle^{-1/2}$ calculated from the vibrational wave functions [5] are significantly smaller, especially at higher vibrational levels. This indicates that the *ab initio* potential is too high at the outer limb of the $\overline{H}$ well, consistent with the trend of the band origins $T_\upsilon$. A more recent *ab initio* calculation of the $H\overline{H}\,^1\Sigma_g^+$ potential gives substantial improvements at

TABLE I. Band origins $T_v$ relative to the $X^1\Sigma_g^+$, $v = 0$, $J = 0$ ground state and rotational constants $B_v$ are fitted to the measured level energies; in parenthesis the uncertainties in the last digit. $\Delta$ indicates deviations of $T_v$ from values calculated in Ref. [5]. The calculated rate of tunneling $P$ through the potential barrier is given for the levels above the ionization potential, and the resulting linewidth $\Gamma$, assuming 100% autoionization efficiency, is given where it exceeds the linewidth due to radiative decay. All values are in $cm^{-1}$ unless stated otherwise.

| $v$ | $T_v$ | $\Delta$ | $B_v$ | $P$ ($s^{-1}$) | $\Gamma$ |
|---|---|---|---|---|---|
| 2 | 123 575.9(1) | −13.6 | 0.97(1) | | |
| 3 | 907.34(3) | −14.11 | 0.962(1) | | |
| 4 | 124 229.63(3) | −14.45 | 0.965(1) | | |
| 5 | 542.75(3) | −14.84 | 0.966(1) | $6 \times 10^{-1}$ | |
| 6 | 846.96(3) | −15.24 | 0.966(1) | $2 \times 10^{1}$ | |
| 7 | 125 142.36(3) | −15.67 | 0.967(1) | $6 \times 10^{2}$ | |
| 8 | 429.15(4) | −16.08 | 0.967(1) | $2 \times 10^{4}$ | |
| 9 | 707.50(4) | −16.48 | 0.970(2) | $3 \times 10^{5}$ | |
| 10 | 977.42(3) | −16.92 | 0.975(5) | $5 \times 10^{6}$ | |
| 11 | 126 238.99(5) | −17.45 | 0.975(5) | $7 \times 10^{7}$ | $3 \times 10^{-4}$ |
| 12 | 492.20(3) | −17.99 | 0.985(1) | $8 \times 10^{8}$ | $4 \times 10^{-3}$ |
| 13 | 736.83(3) | −18.50 | 1.000(1) | $9 \times 10^{9}$ | 0.05 |
| 14 | 972.39(6) | −19.17 | 1.026(5) | $8 \times 10^{10}$ | 0.44 |
| 15 | 127 197.46(4) | −19.62 | 1.097(2) | $7 \times 10^{11}$ | 3.7 |

short internuclear distance; however, it is not reliable at $R \geq 12.5$ a.u., and so it is not useful for calculating improved vibrational energies in the outer well [6].

Information on the decay dynamics of the excited $\overline{H}$ states can be derived from the observed linewidths and the variations in $H_2^+$ and $H^+$ signal strengths. Transitions to vibrational levels with $v \leq 13$ are narrow; line broadening exceeding the laser linewidth was observed only for $v = 14$ and $v = 15$, indicating a shortened lifetime due to autoionization. Under nonsaturation conditions $H_2^+$ is detected only for vibrational levels with $v \geq 12$, increasing with $v$; a strong $H^+$ signal is found for nearly all $v, J$ levels, only for the highest vibrational states it is weak. $H^+$ is not detected unless 355 nm UV radiation is present, whereas the $H_2^+$ yield does not depend on the presence of the UV pulse. This suggests that the $H_2^+$ originates exclusively from autoionization, while $H^+$ is generated when the delayed UV pulse transfers population from the (long-lived) $\overline{H}$ state directly into the dissociation continuum of the ion (see Fig. 1). In cases of significant autoionization, UV-induced dissociation of the $H_2^+$ parent ion may account for the small $H^+$ peak.

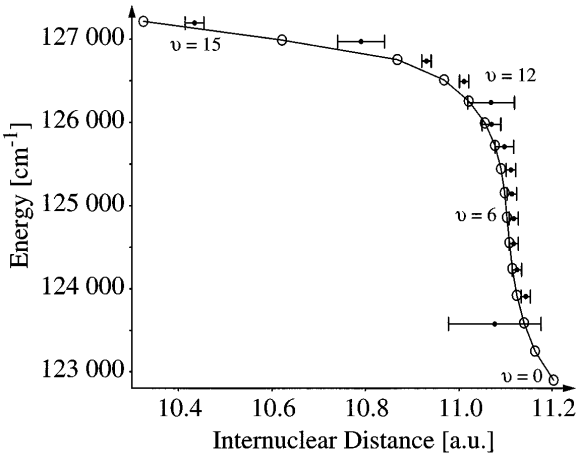


FIG. 3. Mean internuclear distance for $\overline{H}$ (outer well) vibrational states: (∘) $\langle R^{-2}\rangle^{-1/2}$ calculated from vibrational wave functions, Ref. [5]; (•) derived from experimental rotational $B_v$ constants.

Autoionization of $\overline{H}$ states at energies above the ionization threshold, but below the barrier in the $H\overline{H}$ potential, requires tunneling through the barrier to reach the small internuclear distance of the $X^2\Sigma_g^+$ ground state potential of $H_2^+$ at the given energy (cf. Fig. 1). A theory for tunneling in a system governed by an asymmetric double well potential has been developed by Child [10] and applied to the $EF$ system in the hydrogen molecule by Senn and Dressler [3]. In approximation of nonresonant tunneling, the tunneling probability per unit time is given by $P = f_v p(E)$; $f_v$ is the classical oscillation frequency of the vibrational state, which can be derived from the energy difference between neighboring $\overline{H}$ vibrational levels, and $p(E)$ the permeability of the potential barrier at the energy $E$ [3]:

$$p(E) = \exp\left(-2\int\left\{\frac{2\mu}{\hbar^2}[V(R) - E]\right\}^{1/2} dR\right).$$

Here $\mu$ is the reduced mass of $H_2$; the integration is over the classically forbidden region where $V(R) > E$. Based on the *ab initio* $H\overline{H}$ potential from Wolniewicz and Dressler [6] and the experimental energy levels, values for the tunneling rate have been calculated for each vibrational state above the ionization potential ($v \geq 5$) and included in Table I. Also listed are values for the resulting lifetime broadening assuming that autoionization after tunneling is 100% efficient. For $\overline{H}$, $v < 10$ states tunneling rates are smaller than the estimated radiative decay rate of $7 \times 10^6$ $s^{-1}$ [4], so autoionization is effective only in higher vibrational states. For $v \geq 13$ the autoionization lifetime becomes much shorter than the 15 ns delay of the 355 nm pulse, explaining the drop in $H^+$ yield for the highest vibrational states, which is particularly observed for $v = 15$. Observed linewidths fall in intervals of 0.15–0.2 $cm^{-1}$ for $v = 14$ and 0.7–1.5 $cm^{-1}$ for $v = 15$, compared to calculated values of 0.44 and 3.7 $cm^{-1}$, respectively. This can be considered as consistent because autoionization is also influenced by the structure and dynamics of the levels in the inner potential well. In cases where the autoionization efficiency is less than 100% during one classical vibration period in the inner potential well, the ionization rate is lower than the tunneling rate.

Resonant tunneling may occur when states on either side of the potential well are sufficiently close, leading to an enhanced autoionization rate. This effect may

explain the observed strong variations of the $H_2^+$ to $H^+$ peak height ratio as shown in Fig. 4 for $v = 12$, where resonant tunneling to an autoionizing state seems to occur for the $J = 1$ level but not for $J = 3$. Comparable enhanced autoionization was also seen in $v = 13$, $J = 0$, 1, 2, and 4, and in $v = 14$, $J = 0$, 1, 3, and less pronounced in $v = 12$, $J = 5$ and $v = 14$, $J = 4$. In the case of $v = 14$, $J = 3$, and 4, a significant deviation from the fit was found, the $J = 3$ level being shifted upwards and the $J = 4$ level downwards by 0.1 $cm^{-1}$ each, indicating typical behavior expected for resonant tunneling. From the direction of the shifts it follows that, if they are caused by the same state, the perturber state has a larger rotational constant, which is consistent with the fact that it must be localized at short internuclear distance.

In conclusion, we report the observation of an exotic, long-lived, and highly elongated valence state in $H_2$, at an energy near the ionization threshold. In contrast to Rydberg states, which are long-lived and also large in size due to the extended orbital of the Rydberg electron [11], the $\overline{H}$ state owes these properties to its large internuclear separation of 11 times the Bohr radius. Only through a sophisticated double-resonance scheme involving an XUV laser, the $\overline{H}$ state at large internuclear separation could be reached from the ground state. The rotational structure is practically unperturbed, while other states in this energy region are strongly mixed by nonadiabatic interactions and $\Lambda$ uncoupling. Weak autoionization is successfully explained by modeling the nonresonant tunneling through the potential barrier, while resonances strongly enhance the ionization rate of some levels. A number of similar states in hydrogen with $^1\Sigma_g^+$ and $^1\Sigma_u^+$ symmetry are predicted to exist in local potential minima formed by the crossings of H($1s$) + H($nl$) configurations, up to $n = 4$, with the long range Coulomb potential of the $H^+ + H^-$ $(1s)^2$ ion-pair configuration. In contrast to the accurate *ab initio* potential calculations for the $H\overline{H}^1\Sigma_g^+$ and the $B''\overline{B}^1\Sigma_u^+$ states, whose outer minima are formed by the $n = 2$ crossing [6,12], the potentials at the $n = 3$ and $n = 4$ crossings are less well known. For both gerade and ungerade systems a local potential minimum is predicted at an internuclear distance of about 25 a.u. for $n = 3$ and as far out as 200 a.u. for $n = 4$, lying slightly below the ion-pair dissociation energy [13]. Observation of states in these potentials remains a true challenge for further experimental research.

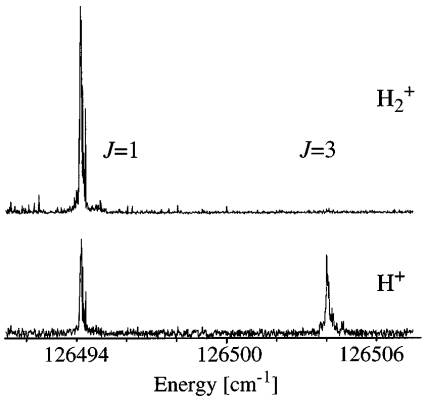


FIG. 4. Resonant tunneling in $\overline{H}$, $v = 12, J = 1$. $H_2^+$ (upper trace) and $H^+$ (lower trace) signals are recorded simultaneously. The $H_2^+$ signal, independent of the delayed UV pulse, is induced by resonant tunneling followed by autoionization and occurring only for $J = 1$ but not for $J = 3$. The $H^+$ signal is induced by the delayed UV pulse, monitoring population of the excited H state.

The authors wish to thank K. Dressler for his suggestion to investigate the $\overline{H}$ state. The Foundation for Fundamental Research of Matter (FOM) and the Vrije Universiteit (USF project grant) are gratefully acknowledged for financial support.

[1] G. DiLinardo and A. E. Douglas, Can. J. Phys. **51**, 434 (1973).
[2] E. R. Davidsson, J. Chem. Phys. **33**, 1577 (1960).
[3] P. Senn and K. Dressler, J. Chem. Phys. **87**, 1205 (1987).
[4] L. Wolniewicz and K. Dressler, J. Mol. Spectrosc. **77**, 286 (1979).
[5] L. Wolniewicz and K. Dressler, J. Chem. Phys. **82**, 3292 (1985).
[6] L. Wolniewicz and K. Dressler, J. Chem. Phys. **100**, 444 (1994).
[7] P. C. Hinnen, W. Hogervorst, S. Stolte, and W. Ubachs, Can. J. Phys. **72**, 1032 (1994).
[8] S. Gerstenkorn and P. Luc, *Atlas du Spectre d'Absorption de la Molécule d'Iode* (CNRS, Paris, 1978).
[9] S. L. Bragg, J. W. Brault, and W. H. Smith, Astrophys. J. **263**, 999 (1982).
[10] M. S. Child, J. Mol. Spectrosc. **53**, 280 (1974).
[11] T. F. Gallagher, *Rydberg Atoms/Cambridge Monographs on Atomic, Molecular and Chemical Physics* (Cambridge University Press, Cambridge, 1994).
[12] W. Kołos, J. Mol. Spectrosc. **62**, 429 (1976).
[13] A. Dalgarno, G. A. Victor, and T. G. Webb, Internal Report No. AFCRL-68-0428 (1968); Internal Report No. AFCRL-70-0551 (1970).